CrossMark

**ORIGINAL PAPER**

# Comparison Between Two Approaches for Non-linear FEM Modelling of the Seismic Behaviour of a Coupled Soil–Structure System

**M. R. Massimino** · **G. Abate** · **S. Corsico** · **R. Louarn**

**Abstract** One basic factor influencing the seismic design of new structures, as well as the retrofitting and/or improvement of existing ones, is the dynamic interaction between the foundation soil and the structure. An accurate investigation of the structure and surrounding soil is the first fundamental step in a realistic evaluation of the seismic performance of the coupled soil–structure system. The present paper deals with the dynamic behaviour of a coupled soil–structure system, i.e. a school building in Catania, characterized by a high seismic hazard. The soil properties were carefully defined by means of in situ and laboratory tests. Different 2D numerical analyses were performed, considering both free-field conditions and the soil–structure interaction (SSI), in order to evaluate quantitatively the known differences between the two types of condition. Seven accelerograms scaled at the same PHA, regarding the estimated seismicity of Catania, were adopted. Two different approaches were used to study soil-nonlinearity, which is extremely important in soil mechanics: firstly, adopting constant degraded shear modula $G$ and increased soil damping ratios $D$, in line with EC8—Part 5 (2003); secondly, choosing $G$ and $D$ according to the effective strain levels obtained for each different input. The main goals of the paper are: (1) to highlight the importance of considering and not considering the dynamic SSI in terms of: acceleration profiles and soil filtering effect; (2) to evaluate the influence of different modelling of soil non-linearity on the dynamic response of the system; (3) to compare the response spectra obtained with that given by the Italian technical code (NTC in New technical standards for buildings, 2008).

M. R. Massimino (✉) · G. Abate · S. Corsico
Department of Civil Engineering and Architecture, University of Catania, Viale Andrea Doria 6, 95125 Catania, Italy
e-mail: mmassimi@dica.unict.it

G. Abate
e-mail: glenda.abate@dica.unict.it

S. Corsico
e-mail: sebastiano.corsico@unict.it

R. Louarn
Geotechnical Design Study "Terrasol", Lyon, France
e-mail: romane.louarn@free.fr

**List of Symbols**

| | |
|---|---|
| $A$ | Amplification function in the frequency domain; i.e. the ratio between the Fourier spectrum at a fixed depth and the Fourier spectrum at the base of the soil deposit |
| $a$, $a_g$ | Acceleration |
| $B$ | Width of the structure |
| $b$ | Coefficient of reduction of the maximum acceleration expected at the site |

🌀 Springer

$BC_1$    Label for boundary condition 1, for all the nodes at the base of the mesh

$BC_2$    Label for boundary condition 2, for all the nodes of the soil vertical boundaries

$c'$    Cohesion of the soil

$C_c$    Parameter depending on the soil type

$C_1$    Coefficient proposed by NTC (2008) for the evaluation of the period of the structure

$D, D(\gamma)$    Damping ratio at the current shear strain $\gamma$

$DSSI$    Dynamic soil–structure interaction

$e_0$    Void ratio

$E$    Young modulus

$E^*$    Degraded Young modulus

$FEM$    Finite element method

$FF$    Free field

$f$    Frequency

$f_{input}$    Frequency of the input

$f_{FF}$    Soil frequency evaluated considering the FF alignment

$f_{SSI}$    Soil frequency evaluated considering the SSI

$F_0$    Seismic parameter: ratio of the spectral acceleration of the constant spectral acceleration branch to the peak ground acceleration

$G, G(\gamma)$    Shear modulus at the current shear strain $\gamma$

$G_0$    Shear modulus at small strains

$G_s$    Specific gravity

$g$    Gravity acceleration

$H$    Height of the soil deposit

$h$    Height of the structure

$I_A$    Intensity of Arias

$K_h$    Horizontal seismic coefficient

$K_v$    Vertical seismic coefficient

$n$    Porosity

$PHA$    Input peak horizontal acceleration

$R_a$    Amplification ratio, i.e. the ratio between the maximum acceleration at a fixed depth and the maximum acceleration at the base of the soil deposit

$RCT$    Resonant column test

$S$    Soil factor by NTC (2008)

$S_a$    Spectral acceleration

$SLO$    Limit state of operability

$SLD$    Limit state of damage limitation

$SLV$    Limit state for life safety

$SLC$    Limit state for collapse prevention

$SDMT$    Seismic dilatometer Marchetti test

$S_S$    Stratigraphic amplification coefficient

$S_T$    Topographical coefficient

$SSI$    Soil–structure interaction

$T$    Period

$T_c$    Seismic parameter: upper limit of the period of the constant spectral acceleration branch

$T_{FB}$    Natural period of the fixed-base structure

$T_{SSI}$    Natural period of the structure including the soil

$T_{STRU}$    Natural period of the structure

$T_{INP}$    Predominant period of the input motion

$U_2$    Displacement in y-direction

$U_3$    Displacement in z-direction

$V_s$    Shear waves velocity

$V_s^*$    Degraded shear wave velocity

$w$    Natural water content

$z$    Vertical axis (depth)

$\alpha$    Rayleigh damping factor

$\beta$    Rayleigh damping factor

$\varphi'$    Angle of shear strength

$\gamma$    Shear strain

$\gamma_{dry}$    Dry unit weight

$v$    Poisson ratio

$\omega$    Angular frequency

# 1 Introduction

Seismic risk assessment is of fundamental importance in a territory like the city of Catania, which is highly subject to severe seismic events. Since seismic risk is a combination of site hazard and vulnerability of the structures, it is of fundamental importance to estimate the seismic input that really impacts the structure accurately, given that this has been shown to change greatly as it propagates from the bedrock to the foundation level, both with reference to the acceleration maximum and the frequency content (Castelli et al. 2008; Grasso et al. 2011; Biondi et al. 2009; Groholski et al. 2010). Therefore, the first step is to use in situ and laboratory geotechnical tests, both in the static and in the dynamic field, to acquire all the geotechnical parameters in the greatest possible detail (Caruso et al. 2016). Studies of coupled soil–structure systems should be consistently encouraged, because without them there is the risk of erroneously

evaluating the seismic response of a structure (Mylonakis et al. 2000; Massimino 2005; Massimino and Scuderi 2009; Pandey et al. 2012; Maugeri et al. 2012; Abate et al. 2016; Massimino and Biondi 2015; Gatto et al. 2015; Abate et al. 2018b). The soil very often has a strategic filtering effect in terms of the maximum acceleration at the foundation level and also in terms of the natural periods of the structures.

Since the 1970s, dynamic SSI has been investigated by means of theoretical approaches (Veletsos and Meek 1974; Gazetas 1983, 1991; Chatterjee and Basu 2008; Voyagaki et al. 2013; Renzi et al. 2013) and numerical modelling (Martin and Houlsby 2001; Gazetas and Apostolou 2004; Gajan et al. 2005, 2008; Massimino, 2005; Maugeri et al. 2012; Calvi et al. 2014; Abate et al. 2015; Abate and Massimino 2017a, b; Behnamfar and Alibabaei 2017) as well as field and laboratory tests (Combescure and Chaudat 2000; Faccioli et al. 2001; Prasad et al. 2004; Kutter and Wilson 2006; Ueng et al. 2006; Bienen et al. 2007; Ugalde et al. 2007; Anastasopoulos et al. 2013; Pitilakis et al. 2018). In particular, numerical modelling of full-coupled soil–structure systems is the most valuable approach, being the nearest to the actual configurations to be analyzed (Abate et al. 2016, 2017).

The present paper deals with the numerical modelling of a full-coupled soil–structure system, i.e. a school building in Catania, characterized by a high seismic hazard (Biondi et al. 2004; Biondi and Maugeri 2005; Grasso and Maugeri 2009a; 2009b). The building and its subsoil were subjected to investigations in the framework of the POR-FESR Research Project Sicilia 2007–2013, which was aimed at reducing the seismic risk in Eastern Sicily (Abate et al. 2018a). The seismic response of a full-coupled system was investigated by means of a 2D FEM modelling, taking into account soil-nonlinearity according to EC8—Part 5 (2003) as well as the strain level reached based on resonant column tests. The results of the full-coupled system analyses were compared with those related to the free-field (FF) site response in the time and frequency domains, in terms of soil amplification ratios, amplification functions and response spectra. The resulting soil amplification ratio and response spectra were also compared with those given by the Italian technical regulations (NTC 2008).

## 2 The Case-History

### 2.1 Description of the Building

This paper deals with an evaluation of the seismic behaviour of the building that hosts the Nazario Sauro school in Catania (Italy), which is characterized by high seismic hazard. The building was designed and built in the period between 1971 and 1975, that is, before Italy was declared a seismic zone in 1982.

Figure 1a shows an axonometric view of the entire building, divided into three volumes indicated as A, A′ and B. Volume B is characterized by an above ground elevation and an underground floor, while the A and A′ volumes have two above ground floors and an underground floor. The entire building is made from reinforced concrete frames which are resistant along the short side in the A–A′ volumes, with resistant frames in the direction of the long side only externally, and in a radial direction in the B volume. In the A and A′ bodies the isolated footings are visible and can therefore be inspected. They have a square truncated pyramidal shape. The two lateral plinths are characterized by a major square base of 2.6 m and a minor rectangular base with sides measuring $0.5 \times 0.7$ m and a height of 1.0 m, while the central plinth has a major square base of 3.0 m and a minor rectangular base measuring $0.55 \times 0.7$ m with a height of 1.2 m. These plinths are placed at a depth of 1.0 m, 1.8 m and 2.6 m respectively from the ground floor. The frame chosen for the SSI analyses is shown in Fig. 1a, b, where the section dimensions and the lengths of the columns and beams are reported.

### 2.2 Geotechnical Characterization of the Foundation Soil

During the design phase in 1971, there was no real geotechnical characterization of the foundation soil, only a geological report according to which the foundation soil was described as a single layer of lava to a depth of 30 m. Hence it was classified as ground type A according to the European technical code (EC8—Part 1 2003) and the Italian technical code (NTC 2018). Moreover, the ground surface is horizontal.

Subsequently a deep geotechnical investigation survey was performed as part of the POR-FESR Project Sicilia 2007–2013 aimed at reducing seismic
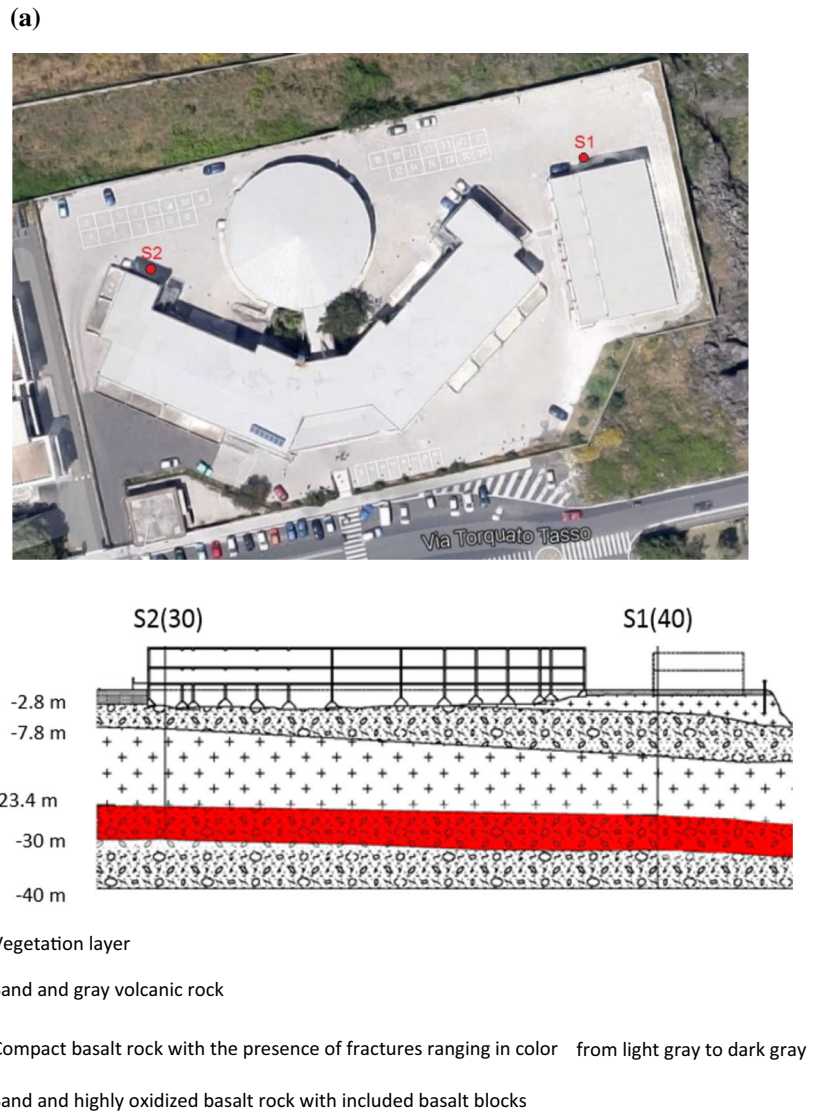
**(a)**



**(b)**
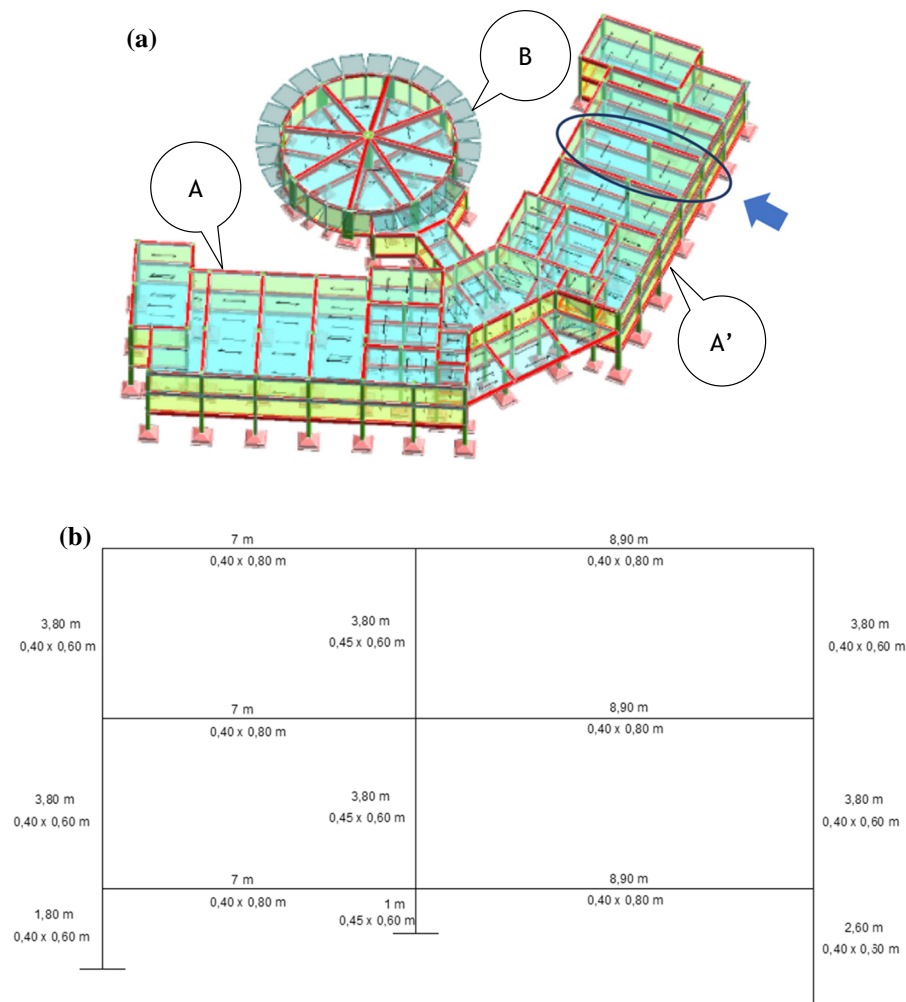


**Fig. 1** School building: **a** isometric view; **b** chosen frame

risk in Eastern Sicily. The soil modelling adopted in the present paper was based on this geotechnical characterization.

Two boreholes, S1 and S2 (Fig. 2), were drilled to a depth of 40 m and 30 m, respectively, from ground level, allowing for a detailed stratigraphy to be performed (Table 1): in the most superficial portion, a vegetation layer rests on an alternation of sand— gray volcanic rock and basaltic rock, deriving from the volcanic eruptions which occurred in Catania in previous centuries; moreover, water was not found within this depth. In addition, two seismic dilatometer tests, indicated as SDMT 2a and SDMT 2b, were performed in the S1 borehole from ground level to depths of 17.5 m and 29.5 m, respectively, obtaining the $V_s$ profiles shown in Fig. 3. The SDMT 2b results

were used in the studies presented here and so three different layers have been adopted for the FEM analyses (the $V_s$ considered in the numerical model is also plotted in Fig. 3), considering the bedrock at a depth equal to 30 m: a first layer, from the ground surface down to 14 m, composed of sand and volcanic debris ($V_s$ = 400 m/s); a second layer, from 14 m to 24 m, composed of fractured basaltic rock ($V_s$ =- 1200 m/s); a third layer, from 24 m to 30 m, composed of sand and volcanic debris ($V_s$ = 800 m/s). From Fig. 3, it is possible to observe consecutive layers of sharply differing stiffness down to a depth of 20 m, and the shear wave velocity of the first layer (0–14 m) is very close to 360 m/s, which is the upper limit of $V_s$ for soil type C; so the foundation soil can be considered of type E as specified by the European

**Fig. 2 a** Location of the
two boreholes; **b** Local
geological model based on
the two boreholes



**(a)**

**(b)**

-2.8 m
-7.8 m
-23.4 m
-30 m
-40 m

S2(30)                                                            S1(40)

Vegetation layer

Sand and gray volcanic rock

Compact basalt rock with the presence of fractures ranging in color   from light gray to dark gray

Sand and highly oxidized basalt rock with included basalt blocks

technical code (EC8—Part 1 2003) and the Italian
technical code (NTC 2018).

A micro-tremor survey (HVSR test) was also
conducted inside the test area to check the seismic
properties of the soil. The maximum depth investi-
gated was equal to 40 m. Figure 4 shows the resulting
H/V profiles vs frequency. By means of this test, the
natural frequency of the soil foundation was evaluated
as approximately equal to 4 Hz.

More detailed information (Table 2) was obtained
thanks to the following laboratory tests: grain size
determination, simple shear tests, uniaxial compres-
sion tests. Resonant column tests were performed at

the Nazario Sauro school site for the layers of sand and
volcanic debris. For the fractured basaltic rock layer,
the $G$–$\gamma$ and $D$–$\gamma$ curves were adopted with reference
to soils characterized by similar $V_s$ values (Fig. 5).

### 2.3 Seismic Inputs

The seismic parameters for the site under examination
(Latitude: 37.511703°–longitude: 15.054803°) are
reported in Table 3 (Soil type E; Topographic cate-
gory T1). Under the Italian technical code (NTC 2008)
the building is classified as class of use III, because it is
a building subject to significant crowding ($C_U = 1.5$).

**Table 1** S1 e S2 profiles

| S2 borehole | | S1 borehole | |
|---|---|---|---|
| Depth (m) | Soil | Depth (m) | Soil |
| 0.00–2.80 | Vegetation layer | 0.00–1.00 | vegetation layer |
| 2.80–7.80 | Sand and gray volcanic rock | 1.00–4.50 | Dark gray compact basalt rock with the presence of fractures |
| 7.80–23.40 | Basalt rock with the presence of fractures ranging in color from light gray to dark gray | 4.50–13.30 | Sand and gray volcanic rock |
| | | 13.30–25.20 | Basalt rock with the presence of fractures ranging in color from light gray to dark gray |
| 23.40–30.00 | "Tufi" with medium-fine yellow–brown grain | 25.20–32.20 | Sand and highly oxidized basalt rock with included basalt blocks |
| | | 32.20–40.00 | Sand and gray volcanic rock |
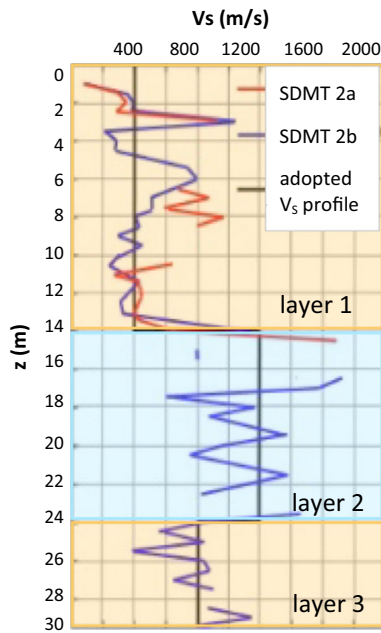


**Fig. 3** *Vs* profiles achieved by SDMT tests
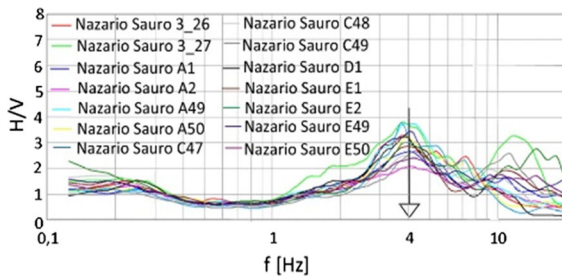


**Fig. 4** Results of the HVSR test

Seven accelerograms were applied to the bedrock of the soil deposit, which was adopted at a depth equal to 30 m as previously described (Sect. 2.2): one input was recorded at the Sortino station during the 1990 Eastern Sicily earthquake, whereas the other six accelerograms were artificial (Fig. 6). The maximum amplitude of all the accelerograms was appropriately scaled to a value equal to $a_g = 0.245$ g, which is the expected value at the bedrock at the site where the school is located, considering the Limit State of Significant Damage (for life safety: SLV; see Table 3). So, the accelerograms used have the same peak acceleration but differ in: (1) frequency content evaluable through the Fourier spectra, as shown in Fig. 6, where the first two fundamental input frequencies $f_{input}(I)$ and $f_{input}(II)$ are reported; (2) significant duration of the earthquake, visible through the Intensity of Arias, $I_A$, referred to the original accelerograms.

## 3 The Full-Coupled FEM Model

The study of the seismic response of the full-coupled soil–structure system was performed by a 2D finite element modelling by means of the ADINA code (ADINA 2008). The response of the system was analyzed both considering and neglecting the SSI by investigating two different vertical alignments: along the structure (SSI) and far from the structure, i.e. free-field condition (FF), as shown in Fig. 7. It is important to stress that the FF alignment was chosen considering

**Table 2** Soil properties achieved by laboratory tests

| Sample | Borehole | Depth (m) | w (%) | $\gamma_{dry}$ (kN/m$^3$) | $G_s$ | $e_0$ | n | Grain size | | Strength | |
|---|---|---|---|---|---|---|---|---|---|---|---|
| | | | | | | | | Gravel (%) | Sand (%) | c′ (kN/m$^2$) | φ′ (°) |
| C1 | S2 | 5–5.5 | 3.76 | 17.2 | 2.74 | 0.65 | 0.39 | 24.28 | 56.07 | 18 | 39 |
| C2 | S1 | 7–7.5 | 8.69 | 16.9 | 2.74 | 0.77 | 0.43 | 51.77 | 41.96 | 20 | 37 |
| C3 | S1 | 11.5–12 | 12.36 | 16.8 | 2.82 | 0.89 | 0.47 | 18.50 | 76.61 | 30 | 37 |

**Fig. 5** $G–\gamma$ and $D–\gamma$ curves adopted for the three soil layers (Curves related to the layer 2 come from RCT performed on soil characterized by similar $V_S$ values)
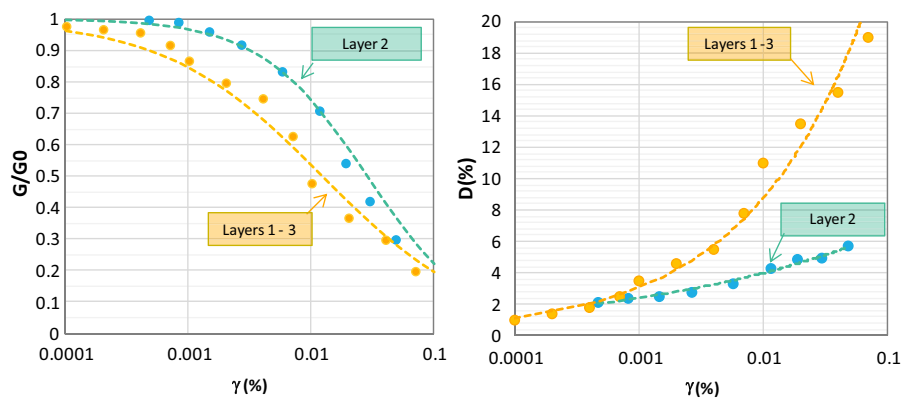


**Table 3** Seismic parameters for the analyzed site

| | $V_R$ (years) | $a_g$ (g) | $F_0$ (–) | $T^*_c$ (s) | $S_s$ (–) | $C_c$ (–) | $S_T$ (–) | $K_h = b*A_{max}/g$ (–) | $K_v = 0.5K_h$ (–) | $a_{max} = a_g xS$ (m/s$^2$) | b (–) |
|---|---|---|---|---|---|---|---|---|---|---|---|
| SLO | 45 | 0.075 | 2.550 | 0.258 | 1.6 | 1.98 | 1 | 0.021 | 0.011 | 1.169 | 0.18 |
| SLD | 75 | 0.092 | 2.518 | 0.277 | 1.6 | 1.92 | 1 | 0.026 | 0.013 | 1.439 | 0.18 |
| SLV | 712 | 0.245 | 2.453 | 0.403 | 1.34 | 1.65 | 1 | 0.102 | 0.051 | 3.213 | 0.31 |
| SLC | 1462 | 0.341 | 2.412 | 0.477 | 1.1 | 1.55 | 1 | 0.116 | 0.058 | 3.676 | 0.31 |

different alignments far from the structure and choosing the one that was not influenced by the vibration of the structure.

Figure 7 shows the mesh used to study the SSI, including the geometry, boundary and loading conditions. The width of the soil deposit was chosen in order to minimize boundary effects as far as possible; the height of the soil deposit was derived from the geotechnical investigations ($H = 30$ m). The model was created according to the hypothesis of plane strain condition. The mesh element size was chosen in order to ensure the following criteria: (1) efficient reproduction of all the waveforms of the whole frequency range under study: $h \leq V_{s,min}/6–8\ f_{max}$ (Lanzo and Silvestri 1999); (2) a finer discretization near the

structure. The frame was modelled by means of 2-node beam elements, with a linear visco-elastic constitutive model characterized by the conventional properties of reinforced concrete ($E = 28500$ MPa, $v = 0.25$, $\gamma = 25$ kN/m$^3$, $D = 5\%$). The soil was modelled by 2D 9-node solid elements, by means of a visco-elastic constitutive model, taking into consideration its non-linear behaviour, which is extremely important in soil mechanics (Abate et al. 2007; Pecker et al. 2010, 2013; Massimino and Biondi 2015). Two different approaches were used to account for soil non-linearity. Firstly, the soil was modelled as a linear equivalent visco-elastic material according to EC8—Part 5 (2003), which suggests degraded shear modula $G$ and increased damping ratios $D$ depending on the
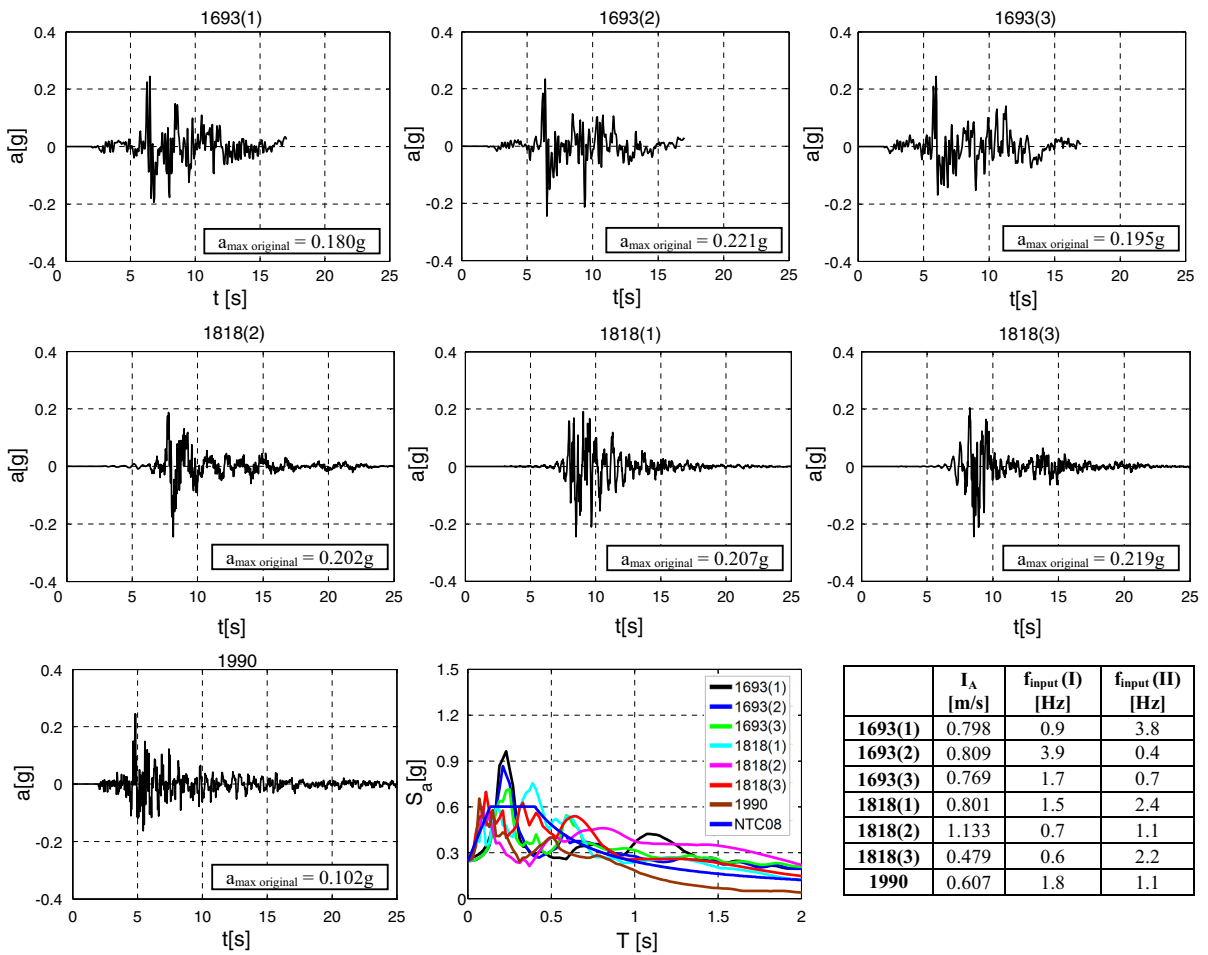
| | $I_A$ [m/s] | $f_{input}$ (I) [Hz] | $f_{input}$ (II) [Hz] |
|---|---|---|---|
| **1693(1)** | 0.798 | 0.9 | 3.8 |
| **1693(2)** | 0.809 | 3.9 | 0.4 |
| **1693(3)** | 0.769 | 1.7 | 0.7 |
| **1818(1)** | 0.801 | 1.5 | 2.4 |
| **1818(2)** | 1.133 | 0.7 | 1.1 |
| **1818(3)** | 0.479 | 0.6 | 2.2 |
| **1990** | 0.607 | 1.8 | 1.1 |

**Fig. 6** Adopted seismic inputs for the FEM analyses
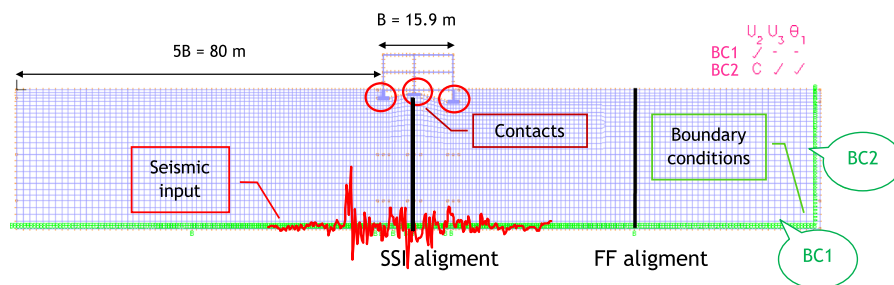


**Fig. 7** Adopted mesh with geometry, boundary and loading conditions

expected surface acceleration for soil types C and D (Table 4), and it suggests a proportionately smaller reduction for stiffer soil profiles, without furnishing precise values of the reduction coefficient. For the case-history analysed, the expected surface acceleration, evaluated as $a_g \times S_S = 0.245 \text{ g} \times 1.34$ (see

Sects. 2.2, 2.3 and Table 3), was greater than 0.3 g; so the degradation and increase in the $G$ and $D$ values adopted are shown in bold in Table 4 and are then specified for the three soil layers in Table 5. In particular, for soil layers 1 and 3 (sand and volcanic debris), the degradation of shear wave velocity was

**Table 4** Values of increasing of $D$ and degradation of $V_s$ and $G_0$ (from Tab.4.1 EC8—Part 5 2003)

| Expected surface acceleration (g) | Damping ratio | $\frac{V_s}{V_{s,max}}$ | $\frac{G}{G_{max}}$ |
|---|---|---|---|
| 0.10 | 0.03 | 0.90(±0.07) | 0.80(±0.10) |
| 0.20 | 0.06 | 0.70(±0.15) | 0.50(±0.20) |
| **0.30** | **0.10** | **0.60(±0.15)** | **0.36(±0.20)** |

**Table 5** Adopted soil characteristics according to "revised" EC8—Part 5 (2003) suggestions

| Soil | Depth (m) | $V_s$* (m/s) | $E$* (MPa) | $v$ | $\gamma$ (kN/m$^3$) | $D$ (%) |
|---|---|---|---|---|---|---|
| Sand and volcanic debris | 0.00–14.00 | $0.60 \cdot V_{smax} = 240$ | 285.9 | 0.3 | 20.3 | 10 |
| Fractured basaltic rock | 14.00–24.00 | $0.75 \cdot V_{smax} = 900$ | 2988.0 | 0.2 | 23.5 | 10 |
| Sand and volcanic debris | 24.00–30.00 | $0.60 \cdot V_{smax} = 480$ | 1231.6 | 0.3 | 21.9 | 10 |

*Degraded values

chosen as equal to $0.60 \cdot V_{smax}$, instead for soil layer 2 (fractured basaltic rock) a minor degradation was chosen ($V_s = 0.75 \cdot V_{smax}$) because it is a stiffer layer. According to the second approach adopted to simulate the nonlinearity of the soil, the values of $G$ and $D$ were chosen according to the $G/G_0$ versus $\gamma$ and $D$ versus $\gamma$ curves shown in Fig. 5, considering the effective strain level $\gamma$ obtained for each soil layer (considering the soil column underneath the structure) and for each different input, according to an iterative sub-routine, as is summarized in Fig. 8. As it is possible to see from Fig. 8, for soil layer 1, the iterative procedure furnished values of $G/G_0$ and $D$ close to the values

fixed by EC8—Part 5; for soil layer 2, due to the very small values of effective strain level $\gamma$, the iterative procedure gave a negligible degradation of the dynamic parameters, different from that suggested by EC8—Part 5; for soil layer 3, the degradation of $G$ and $D$ was less evident than that fixed by EC8—Part 5.

As regards the boundary conditions (labelled as "$BC_1$" and "$BC_2$" in Fig. 7), for all the nodes at the base of the mesh only the horizontal displacements $U_2$ were permitted. Instead, the nodes of the soil vertical boundaries were linked by "constraint equations" that imposed the same displacements $U_2$ and $U_3$ at the
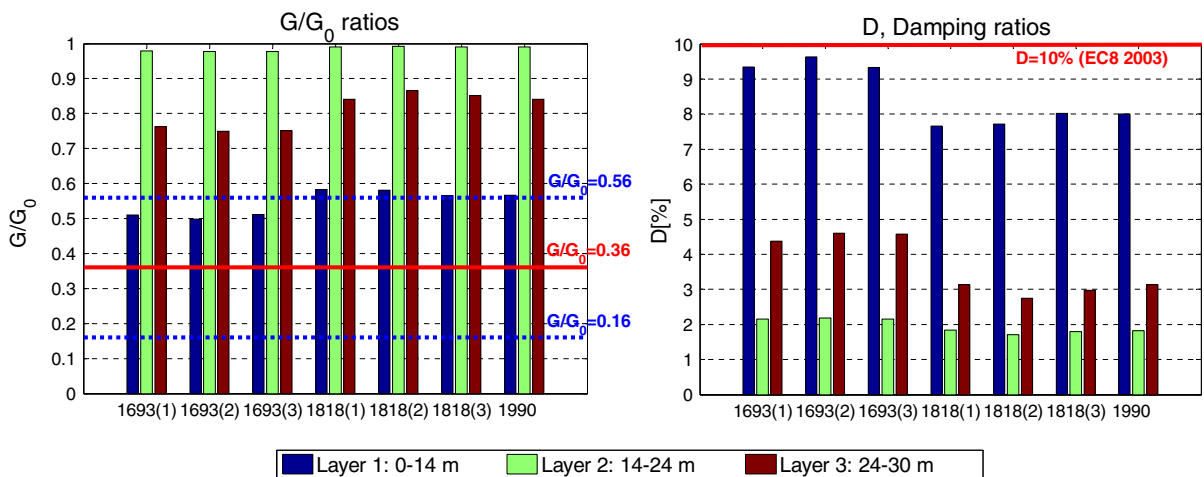


**Fig. 8** Adopted soil characteristics according to the effective strain level

same depths (Abate and Massimino 2016). Special contact surfaces were modelled between the foundations and the soil, considering a friction equal to 2/3 $\varphi$, in order to model probable uplifting and/or sliding phenomena.

As for the loading conditions, the computation of gravitational loads to be applied on the structure was performed as suggested by the Italian technical code (NTC 2008). The loads to be applied to the model were its weight and non-structural loads, considered as concentrated masses on the horizontal beams on the different floors, equal to: 42 kNs$^2$/m and 54 kNs$^2$/m for the separating concrete floors on the 7 m-long beam and 8.9 m-long beam respectively, 30 kNs$^2$/m and 37 kNs$^2$/m for the roof cover on the 7 m-long beam and 8.9 m-long beam respectively. Regarding the input motion, the seven accelerograms shown in Fig. 6, and scaled to the same PHA = 0.245 g as explained in Sect. 2.3, were applied at the base of the model.

The Rayleigh damping factors $\alpha$ and $\beta$ adopted in the numerical modelling for the soil and the structure were computed (Table 6) as $\alpha = D \cdot \omega$ and $\beta = D/\omega$ (Lanzo et al. 2004), being $D$ the damping ratio and $\omega$ the pulsation of the soil or of the structure, computed according to the periods of the systems. The natural frequency of the fixed-base structure was equal to 2.69 Hz, according to the expression: $T = C_1 \ h^{3/4}$ (NTC 2008: $C_1 = 0.075$ is a coefficient proposed for concrete structures); the natural frequency of the soil was equal to 2.95 Hz, according to the well known expression $T = V_s/4H$; see Table 6).

## 4 Results Obtained by the Two Approaches for Soil Nonlinearity Modelling

The seismic response of the soil–structure system to the scenario earthquake expected in the city of Catania is presented here, firstly, following the suggestions in EC8 for soil non-linearity modelling, in terms of:
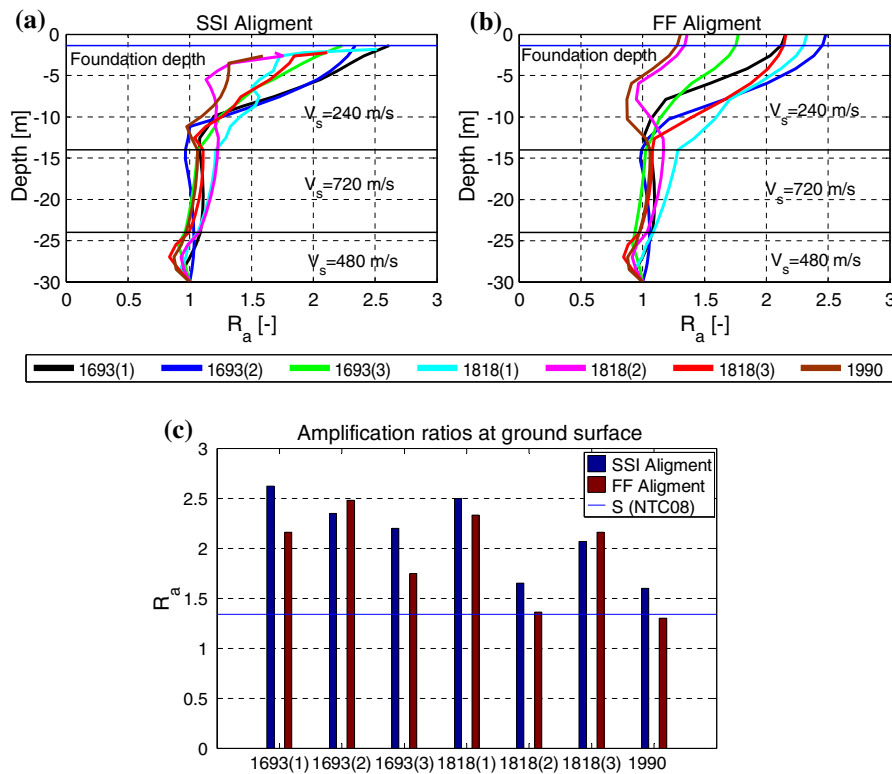
amplification ratio profiles along the two SSI and FF alignments shown in Fig. 7 (Fig. 9a, b) and a comparison between the amplification ratios at the ground surface by the FEM analysis and the Italian technical code (NTC 2008) (Fig. 9c); amplification functions for the two SSI and FF alignments shown in Fig. 7 (Fig. 10a–d); frequency content, as ratios between SSI and FF frequencies (Fig. 10e, f) and ratios between the input frequencies and the soil frequency evaluated considering the SSI (Fig. 11); acceleration response spectra along the SSI alignment (Fig. 12).

Figures 9a, b show the amplification ratios $R_a$ for the seven accelerograms and for the two SSI and FF alignments shown in Fig. 7. The amplification ratio was calculated as the ratio between the maximum acceleration at the depth under consideration and the maximum acceleration at the bedrock. All the accelerograms were subjected to an evident amplification within the shallow layer (10 m below ground surface) with almost vertical trends at deeper layers. The comparison between the alignment under the structure (Fig. 9a) and the free-field condition alignment (Fig. 9b) shows that the presence of the structure generated a strong amplification at the ground surface for the 1990 and 1818(2) accelerograms, which in free-field conditions were subjected to a much lower amplification. Therefore, in these cases it is important to take into account the soil–structure interaction for the seismic safety of buildings. Figure 9c shows the amplification ratios $R_a$ for the seven accelerograms at the ground surface for the two alignments in comparison with the amplification value $S$ calculated by the Italian technical code (NTC 2018) for soil type E and so equal to 1.34 for the SLV (Table 3). It is evident that the values obtained were greater than the value provided by the regulations. The smallest value of $R_a$ was found for the 1990 accelerogram, which was still greater than that provided by NTC (2008).

Figure 10a–d show the amplification functions $A(f)$ for the seven accelerograms and for the two

**Table 6** Evaluation of the Rayleigh damping factors $\alpha$ and $\beta$ for the structure and the soil

|  | $f$ (Hz) | $\omega$ (rad/s) | $D$ | $\alpha$ | $\beta$ |
| --- | --- | --- | --- | --- | --- |
| Structure | 2.69 | 16.88 | 0.05 | 0.844145946 | 0.002961573 |
| Soil | 2.95 | 18.54 | 0.10 | 1.85405 | 0.00539 |

Fig. 9 Amplification ratios for the 7 inputs, achieved according to the first soil non-linearity modeling (EC8 suggestions): **a** along the SSI alignment; **b** along the FF alignment; **c** at the ground surface: comparison with the amplification ratio provided by NTC08

alignments, according to the first and second approaches, respectively. $A(f)$ was evaluated as the ratio between the Fourier amplitude spectrum computed at the foundation level and the Fourier amplitude spectrum computed at the bedrock level, i.e. referring to the soil only, considering both the SSI alignment (Fig. 10a, c) and the FF aligment (Fig. 10b, d).

Considering the first approach for evaluating the soil non-linearity, Fig. 10a shows three natural frequencies of the soil along the SSI alignment equal to: $f_{SSI}(I) = 2$ Hz; $f_{SSI}(II) = 4$ Hz; $f_{SSI}(III) = 5.4$ Hz. The average natural frequency of the soil in free-field condition was about 3.2 Hz (Fig. 10b); this value was similar to the value obtained by the HVSR test (4 Hz), nevertheless there was a slight difference.

Considering the second approach for evaluating the soil non-linearity, Fig. 10c shows three natural frequencies of the soil along the SSI alignment equal to: $f_{SSI}(I) = 2.2$ Hz; $f_{SSI}(II) = 4$ Hz; $f_{SSI}(III) = 5.4$ Hz. These values were very similar to those achieved by the first approach (Fig. 10a). This similarity was due to the predominant role of the structure in the soil

response. The average natural frequency of the soil in free-field condition was 4 Hz (Fig. 10d) and it coincided with that calculated by HVSR.

The different results achieved by the two approaches for taking into account soil non-linearity were due to the rough estimation of the soil non-linearity suggested by EC8—Part 5; the gap was overcome by the second approach, which fixed $G$ and $D$ in relation to the stress–strain level reached.

Figure 10e–f show the ratio between the soil natural frequencies for the SSI alignment ($f_{SSI}(I)$, $f_{SSI}(II)$ and $f_{SSI}(III)$) and the soil natural frequency ($f_{FF}$) for the FF alignment, for each accelerogram and for the two soil non-linearity modelling approaches. It is important to stress that these ratios were often far from unit value. It is very interesting to observe how the natural frequency of the soil was strongly influenced by the presence of the structure. Thus it would not be sufficient to perform site response analyses in FF conditions to estimate the design acceleration of structures.
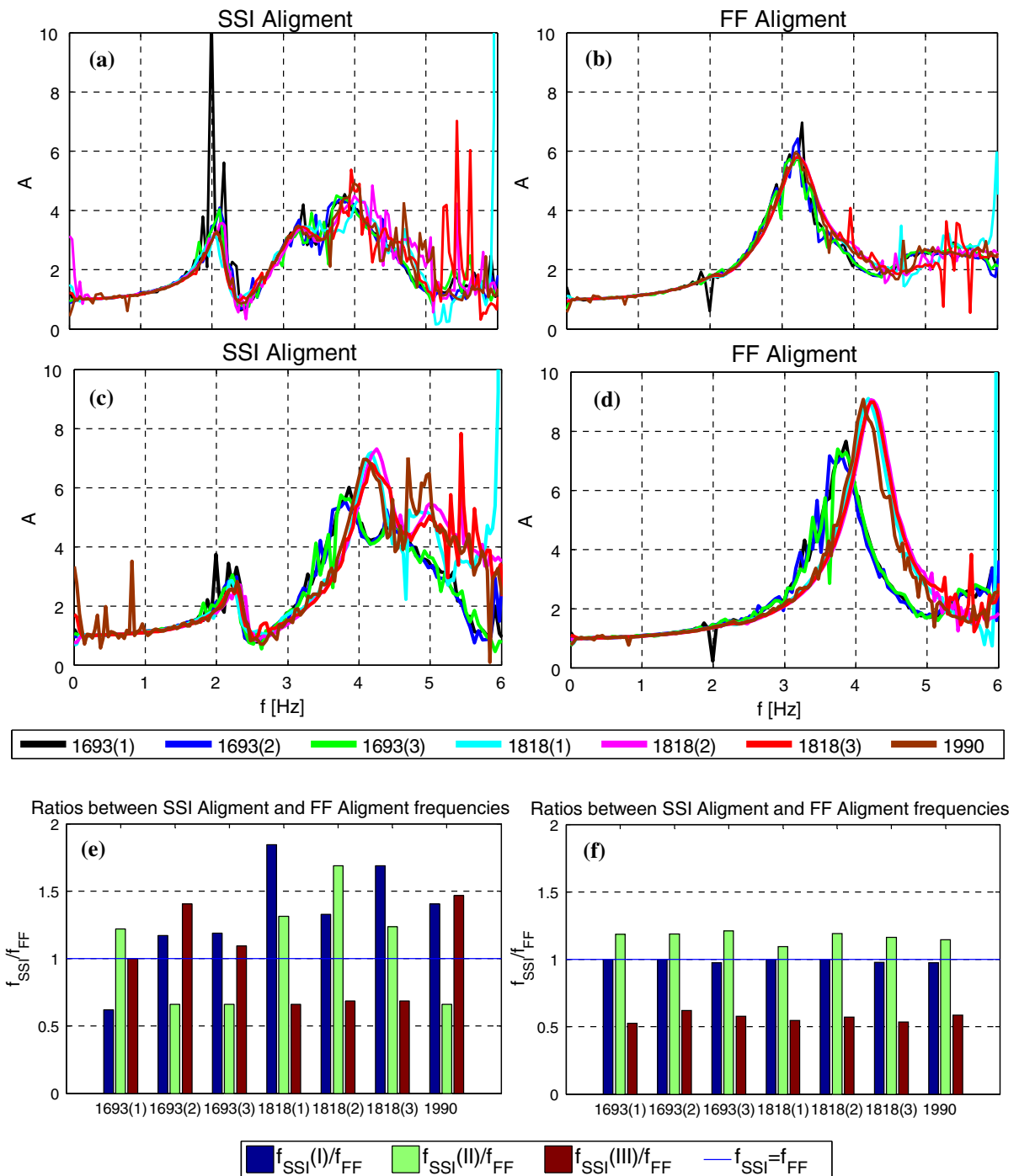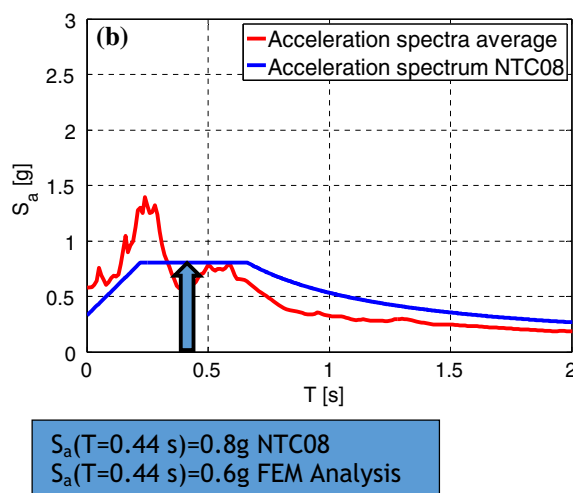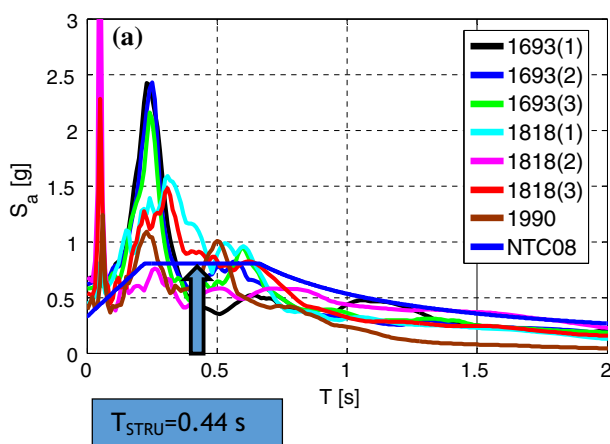
**Fig. 10** Amplification functions for the 7 input: achieved according to first soil non-linearity modeling (EC8 suggestions) along the SSI alignment (**a**) and along the FF alignment (**b**); achieved according to second soil non-linearity modeling (iterative approach) along the SSI alignment (**c**) and along the FF alignment (**d**); ratios between amplification functions for SSI and FF according to first (**e**) and second (**f**) approaches
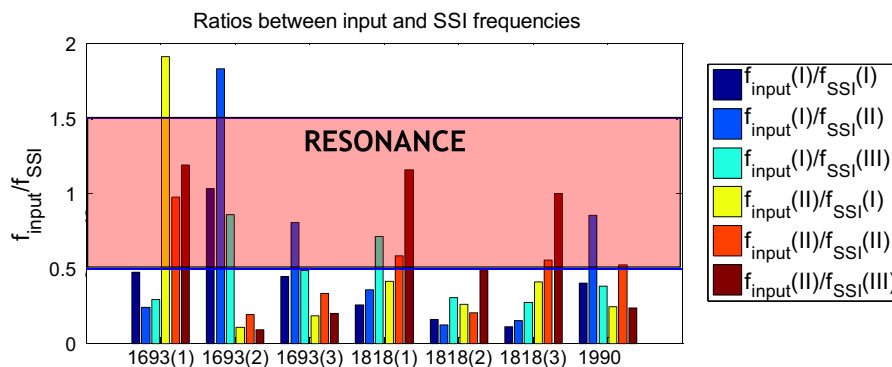
**Fig. 11** Ratios between the fundamental input frequencies and the natural soil frequencies evaluated considering the SSI alignment achieved according to first soil non-linearity modeling (EC8 suggestions): comparison with the frequency ratio range (0.5–1.5) for which resonance phenomena may be



**Fig. 12** **a** Response acceleration spectra for the 7 inputs along the SSI aligment at the foundation level, achieved according to first soil non-linearity modeling (EC8 suggestions); **b** comparison between the acceleration spectra average and the same provided by NTC08, for DSTRU = 5%

Figure 11 shows the ratios between the input frequencies and the soil frequency evaluated considering the SSI, for the first approach adopted for modelling the soil non-linearity (EC8 suggestions). In particular, the first two fundamental input frequencies (Fig. 6) and the first three soil natural frequencies (Fig. 10a) were taken into account. Ratios between 0.5 and 1.5 (within the pink band) indicate the frequency ratios for which there could be resonance phenomena (Sica et al. 2011; Abate and Massimino 2017b); 1693(1), 1693(2) and 1818(1) accelerograms could be considered the most severe, because, for each of them, three of the six $f_{input}/f_{SSI}$ ratios evaluated were in the above-mentioned range, as shown in Fig. 11.

Figure 12 shows the response acceleration spectra along the SSI alignment at the foundation level obtained by the FEM modelling compared with the design spectrum provided by the Italian technical code (NTC 2018). Considering the average of the spectra (Fig. 12b), a spectral acceleration equal to 0.8 g was found for the period of the structure resting on the soil ($T_{stru,SSI}$ = 0.44 s) according to NTC (2008), while a lower value of 0.6 g was obtained from the FEM analysis. Thus, in this case using the NTC 2018 spectra was safer. However, considering a wide range of periods, especially periods approximately equal to 0.25–0.30 s, the FEM spectral acceleration was much larger than that provided by NTC (2008).

SSI had a beneficial effect here, because the natural period of the fixed-base structure ($T_{stru,FB} = 0.37$ s) led to a designed acceleration greater than that required for the natural period of the structure actually resting on the soil ($T_{stru,SSI} = 0.44$ s); even if it is important to stress that in several cases SSI has been shown to have a detrimental effect (Karatzetzou and Pitilakis 2017; Rovithis et al. 2017; Abate et al. 2018a, b).

$T_{stru,FB} = 0.37$ s was evaluated by the amplification function obtained as the ratio between the Fourier amplitude spectra computed at the top and at the bottom of the frame fixed at the base; the same value was found by the modal analysis (see Sect. 3). $T_{stru,SSI} = 0.44$ s was evaluated by the amplification function obtained as the ratio between the Fourier amplitude spectra computed at the top and at the bottom of the frame resting on the soil.

Lastly, the seismic response of the soil–structure system to the scenario earthquakes expected in the city of Catania is presented according to the iterative approach for soil non-linearity modelling, in terms of ratios between the input frequencies and the soil frequency evaluated considering the SSI (Fig. 13); a comparison between the results obtained by the two different approaches for modelling soil non-linearity is shown in Figs. 14 and 15 in terms of amplification ratios and amplification functions along the SSI alignment, respectively.

Figure 13 shows the ratios between the first two fundamental frequencies of the input $f_{input}(I)$ and $f_{input}(II)$ and the first three natural frequencies of the soil along the SSI alignment $f_{SSI}(I)$, $f_{SSI}(II)$ and

$f_{SSI}(III)$, for the iterative approach adopted for modelling the soil non-linearity, similarly to Fig. 11. Once again, the greater severity of the 1693(1), 1693(2) and 1818(1) accelerograms can be noted, because for each accelerogram three of the six $f_{input}/f_{SSI}$ ratios evaluated were in the range of probable resonance.

Figure 14a shows the $R_a$–$z$ profiles and Fig. 14b shows the values of $R_a$ at the ground surface in comparison with the amplification value $S = 1.34$, calculated by the Italian technical code (NTC 2018) for soil type E. As was observed earlier (see Fig. 9b), the values obtained were greater than the value provided by the regulations, and moreover the values obtained by the iterative approach were always greater than the values reached according to those suggested by EC8—Part 5 for soil nonlinearity modelling. This latter result was due to the lower values of $D$ estimated according to the iterative procedure (Fig. 8).
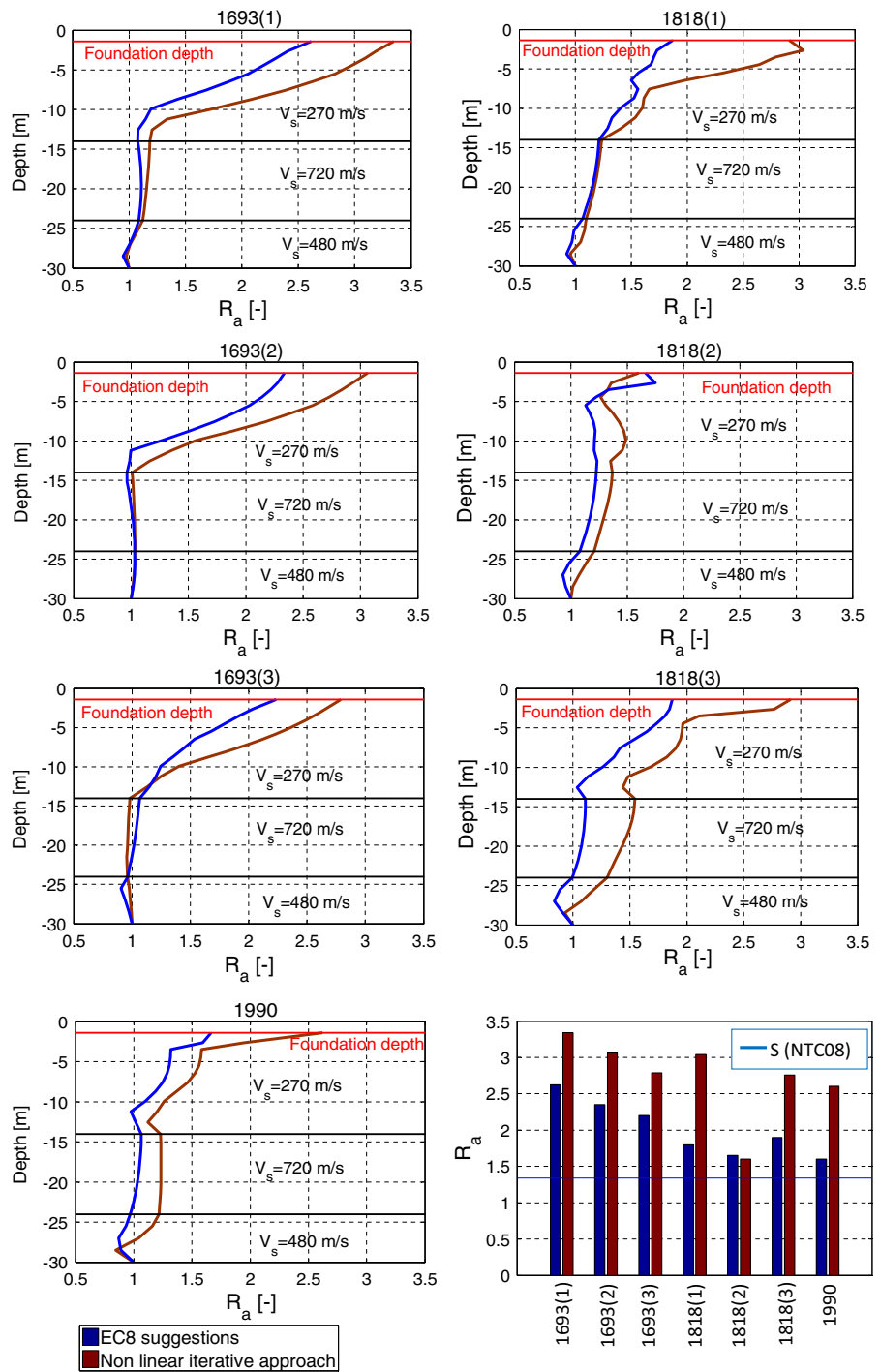
Figure 15 shows the amplification functions for the 7 inputs along the SSI alignment, achieved by both the approaches for modelling soil non-linearity (EC8 suggestions and iterative approach) and evaluated as the ratio between the Fourier amplitude spectrum computed at the foundation level and the Fourier amplitude spectrum computed at the bedrock level. It is possible to observe that modelling soil nonlinearity according to the iterative procedure (red lines), the $A(f)$ peaks move towards greater frequencies, in comparison with the $A(f)$ peaks achieved modelling soil non linearity according to EC8—Part 5 (blue lines). These results were due to higher $G$ values and lower $D$ values estimated according to
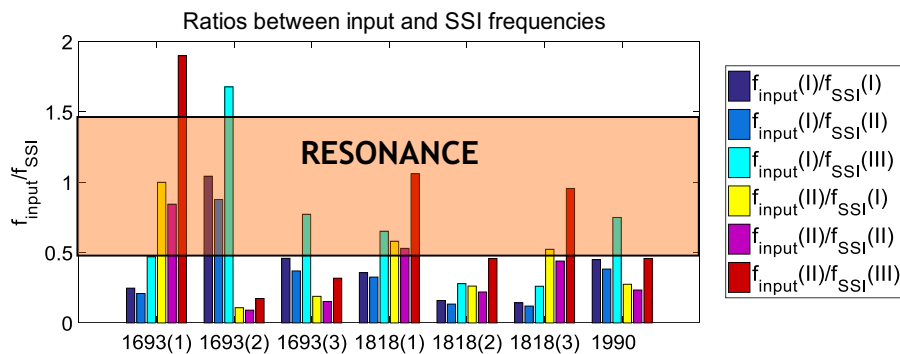


**Fig. 13** Ratios between the fundamental input frequencies and the natural soil frequencies evaluated considering the SSI alignment and achieved according to second soil non-linearity modeling (iterative approach): comparison with the frequency ratio range (0.5–1.5) for which resonance phenomena may be

**Fig. 14** Amplification ratios for the 7 input along the SSI aligment, achieved by the two different approaches to model soil non-linearity (EC8 suggestions and iterative approach): **a** Ra-z profiles; **b** Ra at the ground surface: comparison with the amplification ratio provided by NTC08



the iterative procedure in comparison with those suggested by EC8—Part 5 (Fig. 8). However, the found differences were very small; this is a significant

computational advantage for the designer who wants to take into account soil non-linearity, without adopting onerous procedures.
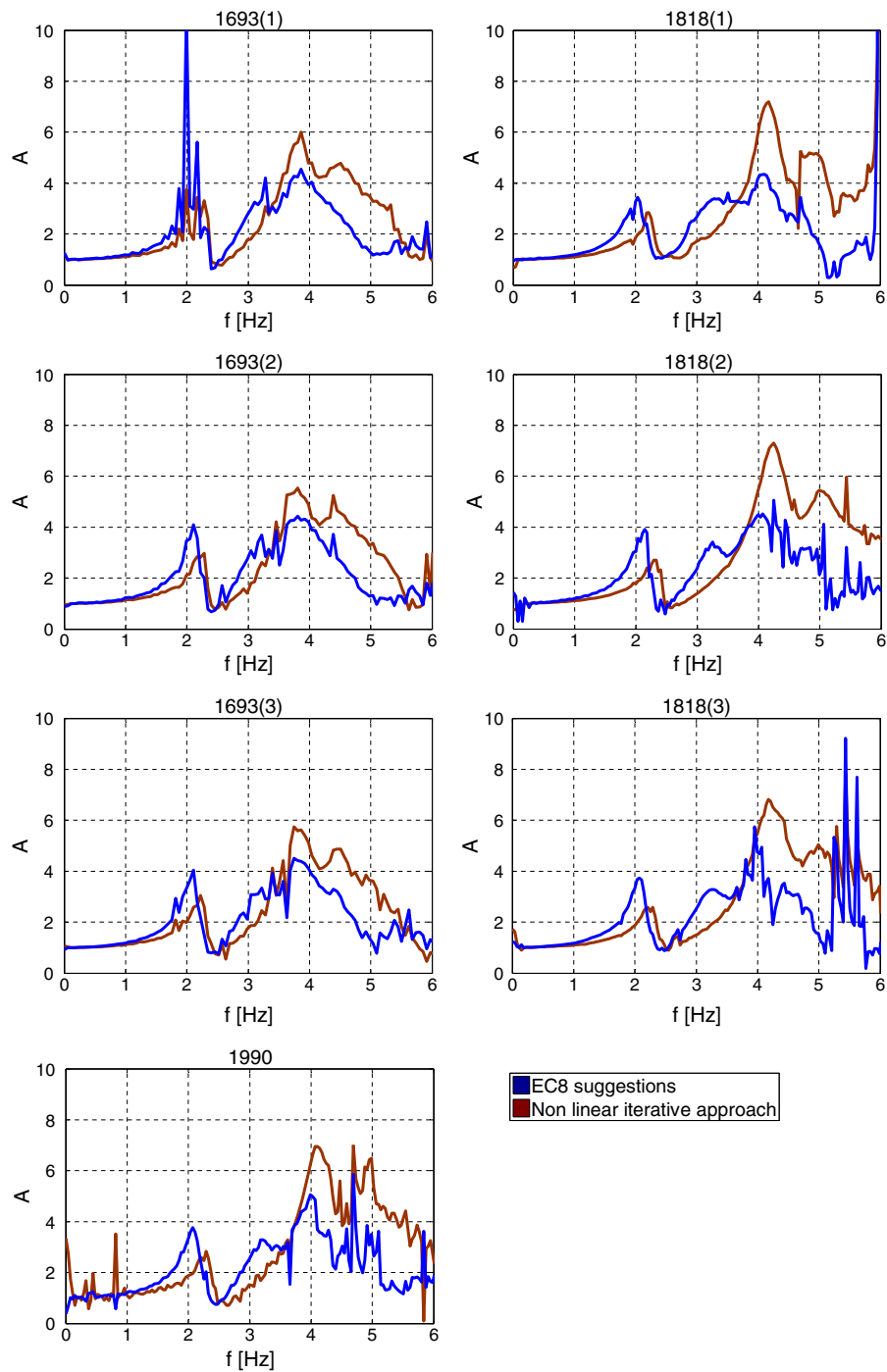
**Fig. 15** Amplification functions for the 7 input along the SSI aligment, achieved by both the approaches for modeling soil non-linearity (EC8 suggestions and iterative approach)

# 5 Conclusions

The present paper reports the 2D FEM modelling of a full-coupled soil–structure system, i.e. a school building in Catania, comparing two different approaches for taking into account soil-nonlinearity: EC8 suggestions regarding the expected acceleration at the ground level and an iterative procedure according to the strain level reached in the soil.

The main results of the study can be summarized as follows.

- A comparison between the alignment under the structure and the free-field condition alignment shows that the presence of the structure generated a strong amplification at the ground surface for some accelerograms (1990 and 1818(2)) which in free-field conditions were subjected to a much lower amplification. This result underlines the importance of taking into account the soil–structure interaction for the seismic safety of buildings.

- The numerical amplification ratios $R_a$ found for the seven accelerograms at the ground surface for the two alignments were greater than the stratigraphic amplification value $S_s$ calculated by the Italian technical code (NTC 2018), and moreover the values obtained by the iterative approach adopted for modelling soil nonlinearity were always higher than the values achieved according to that suggested by EC8—Part 5 (2003) for modelling soil nonlinearity. This latter result was due to the lower values of $D$ estimated according to the iterative procedure.

- The presence of the structure clearly modified the frequency content of the soil, showing basically three soil natural frequencies along the SSI alignment.

- Modelling soil nonlinearity according to the iterative procedure, the $A(f)$ peaks move towards greater frequencies, in comparison with the $A(f)$ peaks achieved modelling soil non linearity according to EC8. These results were due to higher $G$ values and lower $D$ values estimated using the iterative procedure. However, this increase was small, and so a designer who wants to take soil non-linearity into account, without adopting onerous procedures, can advantageously follow the suggestions made by EC8—Part 5 (2003).

- Comparing the ratios between the input frequencies and the soil frequencies (evaluated considering the SSI and obtained using both the approaches adopted for modelling soil non-linearity) with the frequency ratio range which could indicate resonance phenomena, the greater severity of the 1693(1), 1693(2) and 1818(1) accelerograms can be noted.

- A comparison between the numerical response acceleration spectra and the response acceleration spectra provided by the Italian Technical Code shows that, for the period of the structure, the spectral acceleration provided by NTC 2018 is greater than the numerical average spectral acceleration, for both the approaches adopted for modelling soil non-linearity. Thus, it is possible to operate safely according to the regulations, or to design according to the analyses performed and consider a lower spectral acceleration, with consequent optimization of design costs.

- SSI had a beneficial effect in this case because the natural period of the fixed-base structure ($T_{stru,FB} = 0.38$ s) led to a designed acceleration greater than that required for the natural period of the structure actually resting on the soil ($T_{stru,SSI} = 0.44$ s); even if it is important to stress that in several cases SSI has been shown to have a detrimental effect.

- Finally, EC8—Part 5 (2003) suggests an approach which takes into account soil non-linearity only for some types of soils; it also suggests using higher values of $G/G_0$ for stiffer soils than those considered by the regulations, without furnishing precise values. In the analyses, the suggestions made by EC8—Part 5 were adopted for stiffer soils than those considered by the regulations, providing a good comparison with a more rigorous procedure based on the strain levels reached. So the approach based on the EC8—Part 5 suggestions for modelling soil non-linearity is a valid procedure for a routine design.

# References

Abate G, Massimino MR (2016) Dynamic soil–structure interaction analysis by experimental and numerical modelling. Riv Ital Geotecn 50(2):44–70

Abate G, Massimino MR (2017a) Numerical modelling of the seismic response of a tunnel-soil-aboveground building system in Catania (Italy). B Earthq Eng 15(1):469–491

Abate G, Massimino MR (2017b) Parametric analysis of the seismic response of coupled tunnel-soil aboveground building systems by numerical modelling. B Earthq Eng 15(1):443–467

Abate G, Caruso C, Massimino MR, Maugeri M (2007) Validation of a new soil constitutive model for cyclic loading by fem analysis. Solid Mech Appl 146:759–768

Abate G, Massimino MR, Maugeri M (2015) Numerical modelling of centrifuge tests on tunnel–soil systems. B Earthq Eng 13(7):1927–1951

Abate G, Massimino MR, Romano S (2016) Finite element analysis of DSSI effects for a building of strategic importance in Catania (Italy). In: Proceedings of VI Italian conference of researchers in geotechnical engineering—geotechnical engineering in multidisciplinary research: from microscale to regional scale, CNRIG2016. Procedia Engineering, vol 158. pp 374–379

Abate G, Gatto M, Massimino MR, Pitilakis D (2017) Large scale soil-foundation-structure model in Greece: dynamic tests vs FEM simulation. In: Papadrakakis M, Fragiadakis M (eds) Proceedings of 6th ECCOMAS thematic conference on computational methods in structural dynamics and earthquake engineering. COMPDYN 2017. Rhodes Island, Greece, 15–17 June 2017

Abate G, Corsico S, Grasso S, Massimino MR, Motta E (2018a) Dynamic behaviour of coupled soil-structure systems by means of FEM analysis for the seismic risk mitigation of INGV building in Catania (Italy). Ann Geophys. https://doi.org/10.4401/ag-7739

Abate G, Grasso S, Massimino MR, Pitilakis D (2018b) Some aspects of DSSI in the dynamic response of fully-coupled soil-structure systems. Riv Ital Geotecn (to be published)

ADINA (2008) Automatic dynamic incremental nonlinear analysis. Theory and modelling guide. ADINA R&D, Inc., Watertown

Anastasopoulos I, Loli M, Georgarakos T, Drosos V (2013) Shaking table testing of rocking—isolated bridge pier on sand. J Earthq Eng 17:1–32

Behnamfar F, Alibabaei H (2017) Classical and non-classical time history and spectrum analysis of soil–structure interaction systems. B Earthq Eng 15:931–965. https://doi.org/10.1007/s10518-016-9991-7

Bienen B, Gaudin C, Cassidy MJ (2007) Centrifuge tests of shallow footing behavior on sand under combined vertical-torsional loading. Int J Phys Mod Geotech 2:1–21

Biondi G, Maugeri M (2005) Seismic response analysis of Monte Po hill (Catania). WIT Trans State Art Sci Eng. https://doi.org/10.2495/1-84564-004-7/10

Biondi G, Condorelli A, Maugeri M, Mussumeci G (2004) Earthquake-triggered landslides hazard in the Catania area. WIT Trans Ecol Environ. https://doi.org/10.2495/risk040111

Biondi G, Cacciola P, Cascone E (2009) Site response analysis using the Preisach formalism. In: Proceedings of 12th international conference on civil, structural and environmental engineering computing 2009, Madeira, Portugal, 1–4 Sep 2009

Calvi GM, Cecconi M, Paolucci R (2014) Seismic displacement based design of structures: relevance of soil–structure interaction. Geotech Geol Earthq 28:241–275

Caruso S, Ferraro A, Grasso S, Massimino MR (2016) Site response analysis in eastern sicily based on direct and indirect Vs measurements. Proceedings of 1st IMEKO TC4 International Workshop on Metrology for Geotechnics, MetroGeotechnics 2016, Benevento, Italy, 17–18 March 2016, pp 115–120

Castelli F, Lentini V, Maugeri M (2008) One-dimensional seismic analysis of a solid-waste landfill. In: Proceedings of AIP conference, vol 1020, No. 1. pp 509–516

Chatterjee P, Basu B (2008) Some analytical results on lateral dynamic stiffnessfor footings supported on hysteretic soil medium. Soil Dyn Earthq Eng 28(1):36–43

Combescure D, Chaudat T (2000) Icons European program seismic tests on R/C walls with uplift; CAMUS IV specimen. ICONS Project, CEA/DRN/DMT Report, SEMT/EMSI/RT/00-27/4

EC8-Part 1 (2003) Design of structures for earthquake resistance—part 1: GENERAL rules, seismic actions and rules for buildings. ENV 1998, Europ. Com. For Standard, Brussels

EC8-Part 5 (2003) Design of structures for earthquake resistance—part 5: foundations, retaining structures and geotechnical aspects. ENV 1998, Europ. Com. For Standard, Brussels

Faccioli E, Paolucci R, Vivero G (2001) Investigation of seismic soil-footing interaction by large scale cyclic tests and analytical models. In: Special presentation lecture SPL-05, Proceedings of the 4th international conference on recent advances in geotechnical earthquake engineering and soil dynamics. San Diego, USA, 26–31 Mar 2001

Gajan S, Phalen JD, Kutter BL, Hutchinson TC, Martin G (2005) Centrifuge modelling of load deformation behavior of rocking shallow foundations. Soil Dyn Earthq Eng 25(7–10):773–783

Gatto M, Massimino MR, Pitilakis D, Rovithis E (2015) Numerical Simulation of large-scale soil-foundation-structure interaction experiments in the EuroProteas facility. In: Proceedings of 6th international conference on earthquake geotechnical engineering 6ICEGE, 1–4 Nov 2015, Christchurch, New Zealand. Paper N. 401

Gazetas G (1983) Analysis of machine foundation vibrations: state of the art. Soil Dyn Earthq Eng 2(1):2–42

Gazetas G (1991) Foundation vibrations. In: Fang H-Y (ed) Foundation engineering handbook, 2nd edn. Chapman and Hall, New York (Chapter 15)

Gazetas G, Apostolou M (2004) Nonlinear soil–structure interaction: foundation uplifting and soil yielding. In: Proceedings of 3rd UJNR workshop on soil–structure interaction. MenloPark, California, USA (CD-ROM)

Grasso S, Maugeri M (2009a) The road map for seismic risk analysis in a Mediterranean City. Soil Dyn Earthq Eng 29(6):1034–1045

Grasso S, Maugeri M (2009b) The seismic Microzonation of the City of Catania (Italy) for the maximum expected scenario earthquake of January 11, 1693. Soil Dyn Earthq Eng 29(6):953–962

Grasso S, Maugeri M, Monaco P, Totan F, Totani G (2011) Site effects and site amplification due to the 2009 Abruzzo earthquake. WIT Trans Built Environ 120:29–40

Groholski DR, Hashash YMA, Phillips D (2010) Recent advances in non-linear site response analysis. In: Proceedings of 1st international conference on recent advances in geotechnical earthquake engineering and soil dynamics and symposium in honor of Professor I.M. Idriss. May 24–29, 2010. San Diego

Karatzetzou A, Pitilakis D (2017) Modification of dynamic foundation response due to soil–structure interaction. J Earthq Eng. https://doi.org/10.1080/13632469.2016.1264335

Kutter BL, Wilson DL (2006) Physical modelling of dynamic behaviour of soil-foundation-superstructure systems. Int J Phys Mod Geotech 6(1):1–12

Lanzo G, Silvestri F (1999) Risposta sismica locale: teorie ed esperienze. Helvius Edizioni, Napoli

Lanzo G, Pagliaroli A, D'Elia B (2004) Influenza della modellazione di Rayleigh dello smorzamento viscoso nelle analisi di risposta sismica locale. In: Proc. of XI National Conference "Seismic Engineering in Italy" Genova, 25–29 Jan 2004

Martin CM, Houlsby GT (2001) Combined loading of spudcan foundations on clay: numerical modeling. Geotechnique 51(8):687–699

Massimino MR (2005) Experimental and numerical modelling of a scaled soil–structure system. Adv Earthq Eng 14:227–241

Massimino MR, Biondi G (2015) Some experimental evidences on dynamic soil–structure interaction. In: Papadrakakis M, Papadopoulos V, Plevris V (eds) Proceedings of 5th ECCOMAS thematic conference on computational methods in structural dynamics and earthquake engineering, Crete Island, Greece, 25–27 May 2015. COMPDYN 2015, pp 2761–2774

Massimino MR, Scuderi G (2009) Response of a soil–structure system to different seismic inputs. In: Sakr M, Ansal A, TC4 Committee (eds) Proceedings of earth. Geotechnical engineering satellite conference in XVII international conference on soil mechanics and geotechnical engineering October 2–3, 2009, Alexandria (Egypt)

Maugeri M, Abate G, Massimino MR (2012) Soil–structure interaction for seismic improvement of Noto Cathedral (Italy). Geotech Geol Earthq 16:217–239. https://doi.org/10.1007/978-94-007-2060-2_8

Mylonakis G, Gazetas G (2000) Seismic soil-structure interaction: beneficial or detrimental? J Earthq Eng 4(3): 227–301

NTC (2008) D.M. 14/01/08 - New technical standards for buildings, Official Journal of the Italian Republic, 14th January 2008 (In Italian).

NTC (2018) D.M. 17/01/18 - Updating of technical standards for buildings, Official Journal of the Italian Republic, 17th January 2018 (In Italian)

Pandey BH, Liam Finn WD, Ventura CE (2012) Modification of free-field motions by soil-foundation-structure interaction for shallow foundations. Proceedings of 15th World Conference on Earthquake Engineering, Lisbon, 24–28 September, paper 3575

Pecker A, Chatzigogos CT (2010) Non linear soil structure interaction: impact on the seismic response of structures. In: Proceedings of XIV European conference on earthquake engineering. August 2010, Ohrid, FYROM, Keynote lecture

Pecker A, Paolucci R, Chatzigogos CT, Correia AA, Figini R (2013) The role of non-linear dynamic soil-foundation interaction on the seismic response of structures. B Earthq Eng. https://doi.org/10.1007/s10518-013-9457-0

Pitilakis D, Ilioub K, Karatzetzoua A (2018) Shaking table tests on a stone masonry building: modeling and identification of dynamic properties including soil-foundation-structure interaction. Int J Archit Herit. https://doi.org/10.1080/15583058.2018.1431729

Prasad SK, Towhata I, Chandradhara GP, Nanjunaswamy P (2004) Shaking table tests in earthquake geotechnical engineering. Curr Sci India 87(10):1398–1404

Renzi S, Madiai C, Vannucchi G (2013) A simplified empirical method for assessing seismic soil–structure interaction effects on ordinary shear-type buildings. Soil Dyn Earthq Eng 55:100–107

Rovithis E, Kirtas E, Bliziotis D, Maltezos E, Pitilakis D, Makra K, Savvaidis A, Karakostas C, Lekidis K (2017) A LiDAR-aided urban-scale assessment of soil–structure interaction effects: the case of Kalochori residential area (N. Greece). B Earthq Eng. https://doi.org/10.1007/s10518-017-0155-1

Sica S, Mylonakis G, Simonelli AL (2011) Transient kinematic pile bending in two-layer soil. Soil Dyn Earthq Eng 31(7):891–905

Ueng TS, Wang MH, Chen MH, Chen CH, Peng LH (2006) A large biaxial shear box for shaking table test on saturated sand. Geotech Test J 29(1):1–8

Ugalde JA, Kutter BL, Jeremic B, Gajan S (2007) Centrifuge modelling of rocking behaviour of bridges on shallow foundations. In: Proceedings of 4th international conference earthquake geotechnical engineering, Thessaloniki, Greece, June 25–28 (Paper no. 1484)

Veletsos AS, Meek JW (1974) Dynamic behaviour of building-foundation systems. Earthq Eng Struct D 3:121–138

Voyagaki E, Psycharis IN, Mylonakis G (2013) Rocking response and overturning criteria for free standing rigid blocks to single-lobe pulses. Soil Dyn Earthq Eng 46:85–95